Dalton Transactions

Accepted Manuscript

This article can be cited before page numbers have been issued, to do this please use: X. Chen, D. Chen, J. Li, G. Fang, H. Sheng and J. Zhong, *Dalton Trans.*, 2018, DOI: 10.1039/C8DT00430G.

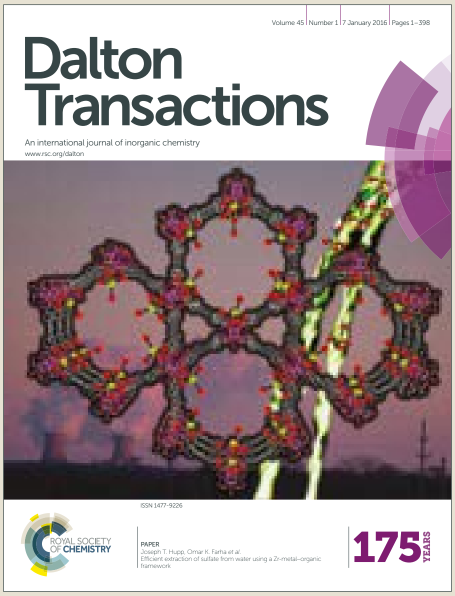

ROYAL SOCIETY OF CHEMISTRY

rsc.li/dalton

View Article Online
DOI: 10.1039/C8DT00430G

Tunable $CsPbBr_3$/Cs_4PbBr_6 Phase Transformation and Their Optical Spectroscopy

Xiao Chen[1], Daqin Chen[1,2] *, Junni Li[1], Gaoliang Fang[1], Hongchao Sheng[3], Jiasong Zhong[1]

[1]College of Materials & Environmental Engineering, Hangzhou Dianzi University, Hangzhou, Zhejiang, 310018, P. R. China

[2]College of Physics and Energy, Fujian Normal University, Fuzhou, Fujian, 350117, P. R. China

[3]Department of Materials Science and Engineering, Jiangsu University of Science and Technology, Zhenjiang, Jiangsu, 212003, P. R. China

*Corresponding author

E-Mail: dqchen@hdu.edu.cn

Fax: (+86)-0571-87713538

View Article Online
DOI: 10.1039/C8DT00430G

ABSTRACT A novel type promising material, metal halides perovskites, is a rising star in optoelectronic field. On this basis, a new frontier of zero-dimensional perovskite-related Cs_4PbBr_6 with bright green emission and high stability has attracted enormous attention, even though its photoluminescence is still required to clarify. Herein, controllable phase transformation between three-dimensional $CsPbBr_3$ and zero-dimensional Cs_4PbBr_6 is easily achieved in a facile ligand-assisted supersaturated recrystallization synthesizing procedure via tuning the amounts of surfactants, and their unique optical properties are investigated and compared in detail. Both Cs_4PbBr_6 and $CsPbBr_3$ produce remarkably intense green luminescence with quantum yields up to 45% and 80%, respectively, but significantly different emitting behaviors can be discerned. Fluorescence lifetime of Cs_4PbBr_6 is much longer than that of $CsPbBr_3$ and photo-blinking is easily detected in the Cs_4PbBr_6 product, proving that zero-dimensional Cs_4PbBr_6 is indeed a highly luminescent perovskite-related material. Additionally, tunable emissions over the visible spectral region are demonstrated to be achievable via halogen composition modulations in Cs_4PbX_6 (X=Cl, Br, I) samples for the first time. Our work brings a simple method for phase control of $CsPbBr_3$/Cs_4PbBr_6 and evidences the intrinsic luminescence nature of zero-dimensional perovskite-related Cs_4PbX_6 products.

Keywords: perovskites; Cs_4PbBr_6; $CsPbBr_3$; quantum dots; luminescence

View Article Online
DOI: 10.1039/C8DT00430G

Introduction

All-inorganic cesium-based perovskite materials have drawn considerable attention for extensive exploration in the fields of photovoltaics,[1-3] display, [4] solar cells,[5-8] lasing[9] and other photoelectric devices because of their superior optical performance and electrical properties. As the optical materials, their diversiform photoluminescence (PL) properties, including wide color gamut, high luminous efficiency, narrow spectral lines and tunable band gap, have pushed their research boom to the forefront.[10-13] The general formula of cesium-based perovskites can be described as Cs_mBX_{2+m}, where B is usually Pb^{2+} or Sn^{2+}, and X^- is the halogen anion (X=Cl, Br or I).[10-15] When m=1, it is the well-known three-dimensional (3D) $CsPbX_3$ perovskite, where PbX_6^{4-} octahedron are corner-shared and Cs^+ ions fill in the voids of PbX_6^{4-} octahedron; when m=4, the perovskite is described as a zero-dimensional (0D) Cs_4PbX_6 one, where PbX_6^{4-} octahedron are separated by Cs^+ cations without sharing X^- anion with each other. Crystals wherein the individual PbX_6^{4-} octahedron are not directly connected to each other are termed as 0D perovskite as the excitons are localized in an isolated octahedron.[16,17] Additionally, two-dimensional (2D) and one-dimensional (1D) structure of perovskites usually presented in the form of nanosheets and nanowires have also been reported.[18-22]

Currently, a small amount of literatures on 0D perovskite-related Cs_4PbBr_6 with appealingly high PL quantum yield (PLQY) have been published.[16-17,23-29] However, the opinions on the PL of Cs_4PbBr_6 are contradictory. Some groups concluded that Cs_4PbBr_6 nanocrystals (NCs, 9~37 nm) did not show any PL within the visible spectral region owing to large band gap (>3.4 eV).[21] Others believed that Cs_4PbBr_6 was highly green luminescence, attributing to the presence of defect states within bandgap such as bromide vacancies serving as radiative recombination centers to capture

DOI: 10.1039/C8DT00430G

excitons.[16,17,24-28] Additionally, only green-emitting Cs_4PbBr_6 was successfully synthesized so far and there is no report on blue and red luminescence of Cs_4PbX_6 (X=Cl/Br or Br/I) as far as we know.

A variety number of solution-processed methods are available for the preparation of these perovskites materials so far, such as hot injection, ligand-assisted supersaturated recrystallization (LASR), solvothermal route and even ultrasonication.[10-13, 30-33] Herein, we realize the controllable synthesis of 3D perovskite $CsPbX_3$ NCs and 0D perovskite-related Cs_4PbX_6 particles through a modified LASR strategy. The fabrication was operated at room temperature (RT) via supersaturated recrystallization in a few seconds, being activated by transferring Cs^+, Pb^{2+}, and X^- precursor ions from a soluble solvent to an insoluble one. Importantly, it is demonstrated for the first time that the products can completely transform from monoclinic 3D $CsPbX_3$ phase to hexagonal 0D Cs_4PbX_6 one as the amounts of surface ligands change. PL, PL excitation (PLE), time-resolved fluorescence spectra and single-particle fluorescence images have been adopted to systematically compare their optical performance, certainly confirming the intrinsic luminescent nature of the prepared Cs_4PbX_6 particles. Importantly, not limited to $CsPbX_3$ NCs, 0D structure perovskite-related Cs_4PbX_6 can also achieve the spectral shift by changing halogen element. It is a great significance for the future application of these 0D structure perovskite-related Cs_4PbX_6 in the optoelectronic field.

Experimental Section

Materials and Chemicals. Lead chloride ($PbCl_2$, 99.99%; Aladdin), lead bromide ($PbBr_2$, 99.0%; Macklin), lead iodide (PbI_2, 99.9%; Aladdin), cesium bromide (CsBr, 99.5%; Macklin), oleic acid (OA, 90%; Aldrich), oleylamine (OM, 80~90%; Aldrich), dimethylformamide (DMF, 99.5%;

View Article Online
DOI: 10.1039/C8DT00430G

Macklin), dimethyl sulfoxide (DMSO, 99.5%; Macklin), and toluene (C_7H_8, 99.0%; Macklin) were used as received without further purification.

Synthesis of $CsPbX_3$ NCs. In a typical synthesis of $CsPbBr_3$ NCs, $PbBr_2$ (0.4 mmol), CsBr (0.4 mmol) were dissolved in a DMF (DMSO for dissolving $PbCl_2$ in synthesis of $CsPb(BrCl)_3$ NCs) solution (10 mL). DMF or DMSO acts as a good solvent to dissolve inorganic salts and small molecules. After complete dissolution, OA (0.1 ml) and OM (0.2ml) were added to stabilize the precursor solution. Then, 0.4 mL of the precursor solution was quickly injected into 10 mL of toluene (bad solvent) to induce $CsPbBr_3$ crystallization via vigorous stirring. Bright green emission was immediately observed after the injection. Other samples with different emission colors were fabricated with a mixture of stoichiometric amounts of PbX_2 (X = Cl, Br, I) by a similar procedure. All of the above operations were implemented at room temperature, which varies with seasons from ~0 °C in the winter of Hangzhou to ~30 °C in the summer of Hangzhou.

Synthesis of Cs_4PbX_6 particles. The step of Cs_4PbX_6 NCs is similar to the synthesis of $CsPbX_3$ NCs. The only different is that more surfactant (2.5 ml OA and 1.25ml OM) are needed to stabilize the precursor solution to get Cs_4PbX_6 product.

Characterization. X-ray diffraction (XRD) analysis was carried out to identify the phase structure of the as-prepared samples using a powder diffractometer (MiniFlex600 RIGAKU) with Cu K_α radiation (λ=0.154 nm) operating at 40 kV. Field emission scanning electron microscope (FESEM, JSM-6700F) equipped with energy dispersive X-ray spectroscopy (EDS) system was carried out to investigate microstructures and actual composition of samples. Fourier transform infrared spectra were recorded on a Nicolet 6700 FTIR spectrometer in the range of 4000~400 cm^{-1} using the KBr pellet technique. Absorption and photoluminescence (PL) spectra were recorded on an Edinburgh Instruments FS5 spectrofluorometer equipped with continuous (150 W) and pulsed xenon lamps. Excitation-emission mappings of the products were recorded on the FS5 spectrofluorometer by continuously changing excitation wavelength with a fixed step of 1 nm, and the offset between excitation wavelength and emission one was set to be 30 nm to reduce scattering light. Time-resolved spectra of the NCs were detected on a fluorescent lifetime spectrometer (LifeSpec-II; Edinburgh Instruments) based on a time correlated DT-ART-01-2018-000038single-photon-counting technique under excitation with a 375 nm picosecond laser. Photoluminescence quantum yield (PLQY), defined as the ratio of emitted photons to absorbed ones, was determined by a spectrofluorometer (FS5) equipped with an 15 cm integrating sphere and the xenon lamp as the excitation source (λ_{ex}=375 nm). For the single particle emission observation, PL measurements were conducted on a home-built Raman/PL system, consisting of an inverted microscope (Ti eclipse, Nikon) and a Raman spectrometer (iHR320, Horiba) attached with an CCD detector (Syncerity, Horiba). A 405 nm laser was focused onto the sample using a 100×, 0.95 NA objective lens (Olympus) and then PL images were recorded by a visual camera.

Results and Discussion

3D perovskite $CsPbBr_3$ and 0D perovskite-related Cs_4PbBr_6 were synthesized through a well-known LASR strategy, which is operated at RT and finished within few seconds through transferring the Cs^+, Pb^{2+}, and Br^- ions from soluble to insoluble solvents (**Figure 1a**). Typically, for fabricating $CsPbBr_3$ NCs, a 10 mL dimethylformamide (DMF) solution of CsBr (0.4 mmol) and $PbBr_2$ (0.4 mmol) with 0.2 mL oleylamine (OM) and 0.1 mL oleic acid (OA) was firstly prepared. Then, appropriate amount of the precursor (0.25 mL) was dropwise added into toluene

View Article Online
DOI: 10.1039/C8DT00430G

(10 mL) under vigorous stirring, and bright green luminescence was immediately observed after the injection. The dropping procedure induced a highly supersaturated state and then led to fast crystallization of $CsPbBr_3$ NCs. The only difference for preparing Cs_4PbBr_6 particles is that more surface ligands (2.5 mL OM and 1.25 mL OA) are needed to configure the precursor solution. The distinct differences can be observed that the precursor for forming Cs_4PbBr_6 presents emulsion, on the contrary, clear precursor solution for forming $CsPbBr_3$ NCs is in stark contrast to the former (**Figure 1a**). Notably, the prepared $CsPbBr_3$ and Cs_4PbBr_6 samples show high PLQYs of 80.6% and 45.7%, respectively (**Figure S1**). In this synthetic system, the amount of surface ligands has a great influence on the phase structures of products. X-ray diffraction (XRD) patterns of products synthesized by the different contents of surfactants in precursor solution are shown in the **Figure 1b**. When the surfactant content is low in the precursor solution, the resulting product is pure 3D structured perovskite $CsPbBr_3$ (JPCDS No. 18-0364); when the surfactant content is high enough,

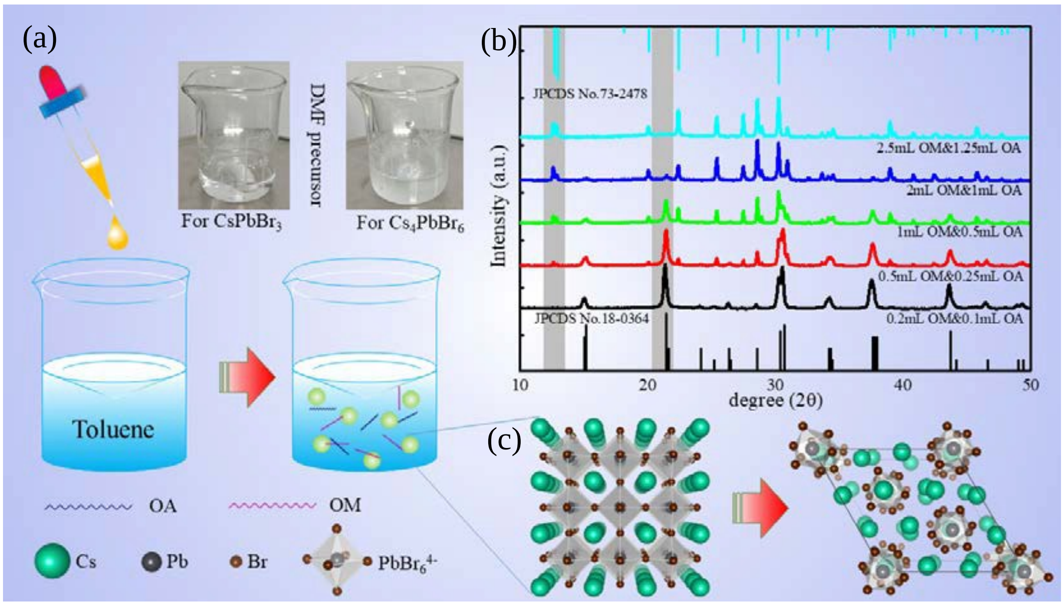

Figure 1. (a) Schematic illustration of the synthesis procedure for $CsPbBr_3$ and Cs_4PbBr_6 via a LASR route. (b) XRD patterns of the synthesized products obtained by using different amounts of OA and OM surfactants. Bars are standard diffraction data of monoclinic $CsPbBr_3$ (JPCDS No. 18-0364) and hexagonal Cs_4PbBr_6 (JPCDS No. 73-2478) crystals. (c) Crystal structures of 3D $CsPbBr_3$ and 0D Cs_4PbBr_6, where green, grey and dark red spheres represent Cs^+, Pb^{2+} and Br^- ions, respectively.

View Article Online
DOI: 10.1039/C8DT00430G

the precursor becomes white emulsion and the crystallize phase is evidenced to be pure 0D perovskite-related Cs_4PbBr_6 (JPCDS No. 73-2478). If the amount of surfactant content is between them, $CsPbBr_3$ and Cs_4PbBr_6 hybrid phases can be obtained. The crystal structures of $CsPbBr_3$ and Cs_4PbBr_6 are schematically illustrated in **Figure 1c**. Apparently, $PbBr_6^{4-}$ octahedral units are corner-shared in 3D perovskite $CsPbBr_3$ while they are spatially isolated by Cs^+ ions in 0D perovskite-related Cs_4PbBr_6.

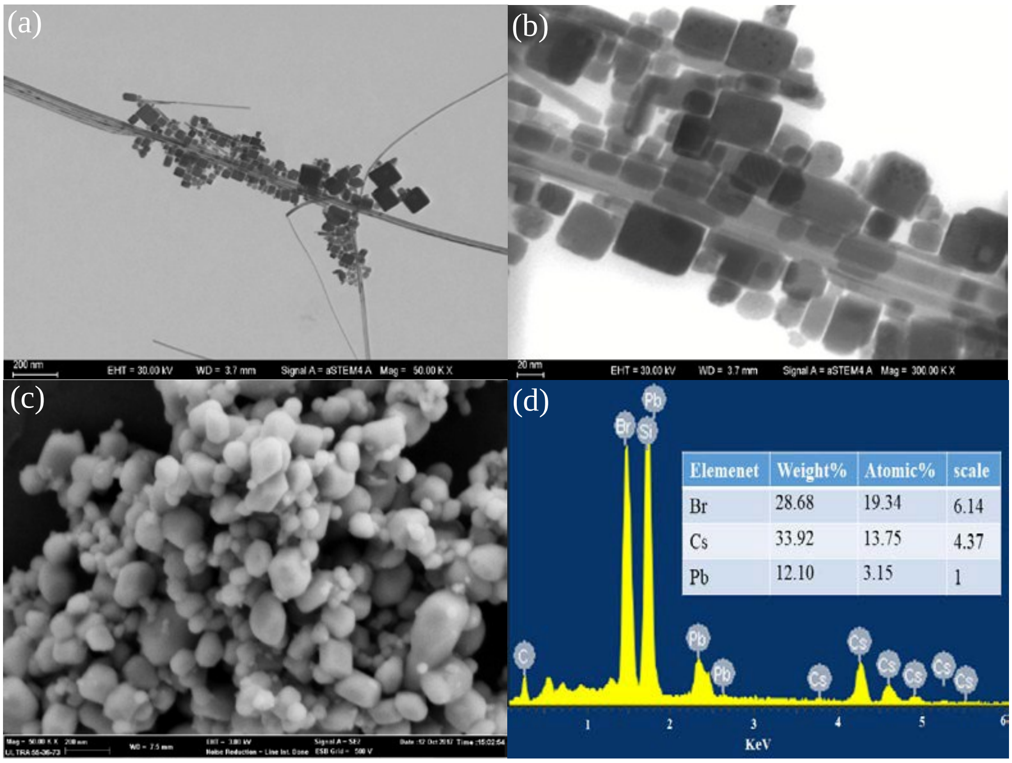

Elemenet	Weight%	Atomic%	scale
Br	28.68	19.34	6.14
Cs	33.92	13.75	4.37
Pb	12.10	3.15	1

Figure 2. Typical FESEM images of (a, b) $CsPbBr_3$ and (c) Cs_4PbBr_6 particles. (d) EDS spectrum of Cs_4PbBr_6 NCs and the tabulated Cs, Pb, Br contents, showing Cs:Pb:Br ratio being close to 4:1:6.

Field emission scanning electron microscope (FESEM) images evidence that the $CsPbBr_3$ product exhibits regular cuboid with sizes of 10~20 nm (**Figure 2a**, **2b**) and the Cs_4PbBr_6 sample shows irregular morphology with sizes of 50~200 nm (**Figure 2c**). Elemental analyses by energy dispersive spectrometer (EDS) demonstrates the approximate atomic ratio of Cs:Pb:Br=4:1:6 for the Cs_4PbBr_6 sample (**Figure 2d**). The Br: Pb ratio is determined to be 6.14:1 and is larger than the normal one based on the chemical formula of Cs_4PbBr_6, indicating the formation of Br-rich

View Article Online
DOI: 10.1039/C8DT00430G

surfaces in Cs_4PbBr_6. A similar phenomenon was also reported in other metal-halide perovskites such as $CsPbBr_3$ quantum dots.[11]

Figure S2 show the PL/Absorption spectra of pure $CsPbBr_3$, Cs_4PbBr_6 products and their mixtures. A sharp PL band located around 520 nm with full width at half maximum (FWHM) of ~100 meV was detected for pure $CsPbBr_3$ NCs, and an absorption band edge at 515 nm with Stokes shift of 15 meV related to PL band is observed in the UV-visible absorption spectrum (**Figure S2a**), indicating the direct exciton recombination luminescence of $CsPbBr_3$. Impressively, with gradual conversion from $CsPbBr_3$ to Cs_4PbBr_6, both absorption and PL band show blue-shift, i.e., move towards short-wavelength, without remarkable modification of the related FWHMs. As exhibited in **Figure S2b**, the corresponding time-resolved PL spectra were recorded to understand their exciton recombination dynamics. The average decay lifetimes are determined based on the equation of $\tau_{\text{ave}} = \int I(t)dt / I_p$ due to their non-single-exponential feature, where $I(t)$ is the time-dependent emission intensity, and I_p the peak intensity in the decay curve. PL lifetime of pure $CsPbBr_3$ (5.9 ns) is far shorter than that of pure Cs_4PbBr_6 (13.1 ns) and gradually increases with phase transformation from $CsPbBr_3$ to Cs_4PbBr_6. Furthermore, time and temperature dependent emission behaviors were investigated in the revised manuscript. No obvious change for emission intensity of both phases was found with increase of storing time up to 14 days and gradual decrease of emission intensity was observed when recording temperature was elevated from 83 K to 383 K (Figure S3). In order to verify the repeatability of this phenomenon, the optical properties by varying the ratio of the proportion of halogen in the precursor (for example, Br/Cl=2:1) were further studied, and similar results were obtained, as demonstrated in **Figure S4**. Phase transition from $CsPb(Br/Cl)_3$ to $Cs_4Pb(Br/Cl)_6$ will also induce blue-shift of PL band from

View Article Online
DOI: 10.1039/C8DT00430G

485 nm to 468 nm and prolong PL lifetime from 4.3 ns to 12.3 ns.

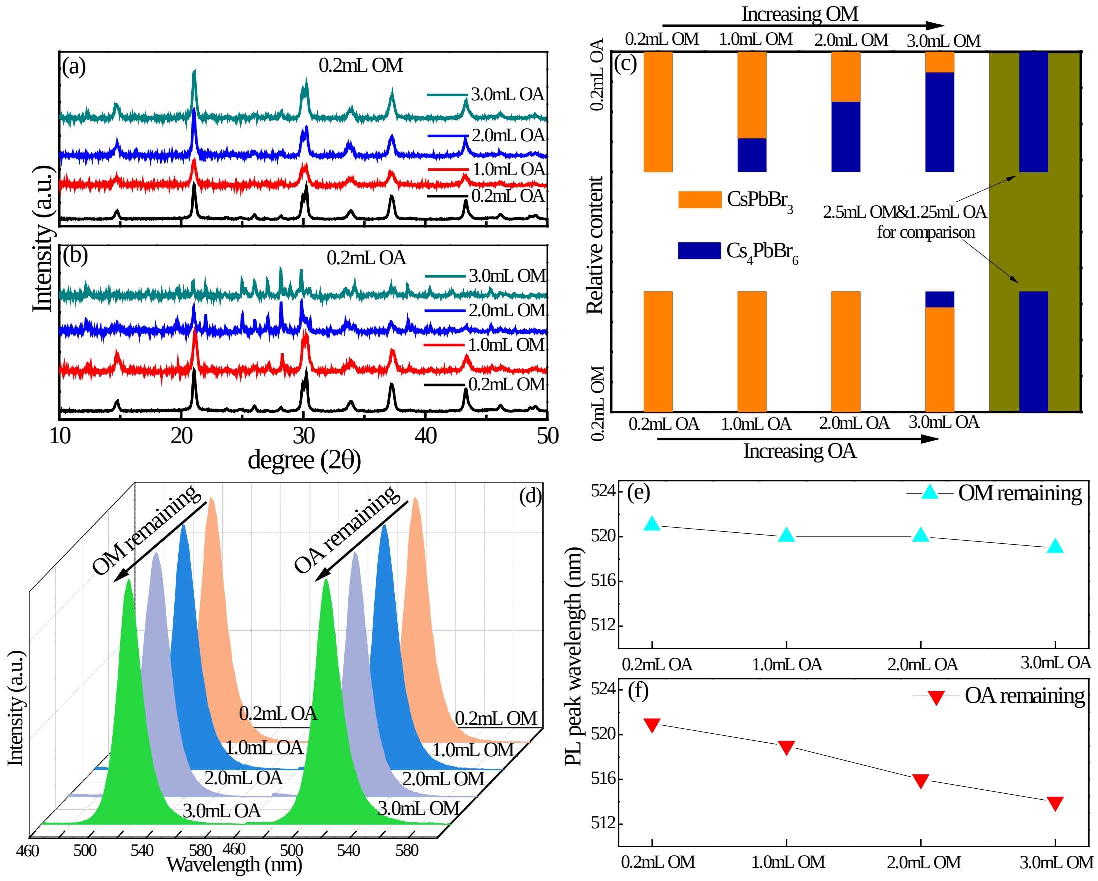

Figure 3. XRD patterns of the products synthesized by using different amounts of surfactants with (a) fixed OM content (0.2 mL) and (b) fixed OA content (0.2 mL). Dependence of (c) relative content of $CsPbBr_3$ and Cs_4PbBr_6 products, (d) PL spectra, (e, f) PL peak wavelength on OA&OM contents.

As aforementioned, one of the fundamental issues that needs to be addressed is which surface ligand, OA or OM, plays a more important role in phase transition. Actually, many literatures reported on the role of surfactants in the formation of NCs,[34-37] but the influence of the surfactants on the phase transformation was seldom studied.[38] Adopting ingenious designed experiments, control variable method is the most feasible scheme to explore the influence of different surfactants on the crystalline phase. When OM content is fixed to 0.2 mL, only a small amount of 0D perovskite-related Cs_4PbBr_6 emerge even after increasing OA content up to 3 mL (**Figure 3a**, **3c**). However, when OA content is set to 0.2 mL, only 1mL OM are required to trigger the growth of Cs_4PbBr_6 and the products are almost pure Cs_4PbBr_6 with the addition of 3 mL OM (**Figure 3b**,

View Article Online
DOI: 10.1039/C8DT00430G

3c). Notably, the relative content of $CsPbBr_3$ and Cs_4PbBr_6 is estimated by the ratio of the integrated area of the diffraction peaks assigned to $CsPbBr_3$ phase and Cs_4PbBr_6 one, respectively. Correspondingly, PL spectra (**Figure 3d**) evidence obvious difference of the displacement of the emission peak wavelength (**Figure 3e**, **3f**), indicating that OM plays an important role for the production of 0D perovskite-related Cs_4PbBr_6. For a detailed discussion of what role does surfactant (OA&OM) play in the formation of Cs_4PbBr_6, we refer to a few recent review articles reported by Liberato Manna and Liu Yang, respectively.[23,39] Such synthetic systems for forming Cs_4PbBr_6 that uses OA and OM all appear a similar phenomenon that a lot of surfactants are needed in comparison with $CsPbBr_3$. It is also known that long hydrocarbon molecules containing a coordinating head-group (OA with COOH group, OM with NH_2 group) as ligands which sterically stabilize NCs in nonpolar and hydrophobic solvents as well as play a key role in the self-assembly of ordered NC arrays. As evidenced in **Figure S5**, the amounts of NH_2 and COOH groups on the surface of Cs_4PbBr_6 particles are far more than those on the surface of $CsPbBr_3$. Steric hindrance increases with rise of OA&OM content in the precursor solution, so that the PbX_6^{4-} octahedrons are hard to get together to produce a three-dimensional structure. As for the role of OM being greater than that of OA, herein we propose a hypothesis that head-group of amino in OM is easy to attract positively charged Cs^+ ions due to a lone-pair electrons on the nitrogen atom.[40] These assembled cesium ions tend to separate the PbX_6^{4-} octahedrons and 0D structured Cs_4PbBr_6 is thus more likely to form.

View Article Online
DOI: 10.1039/C8DT00430G

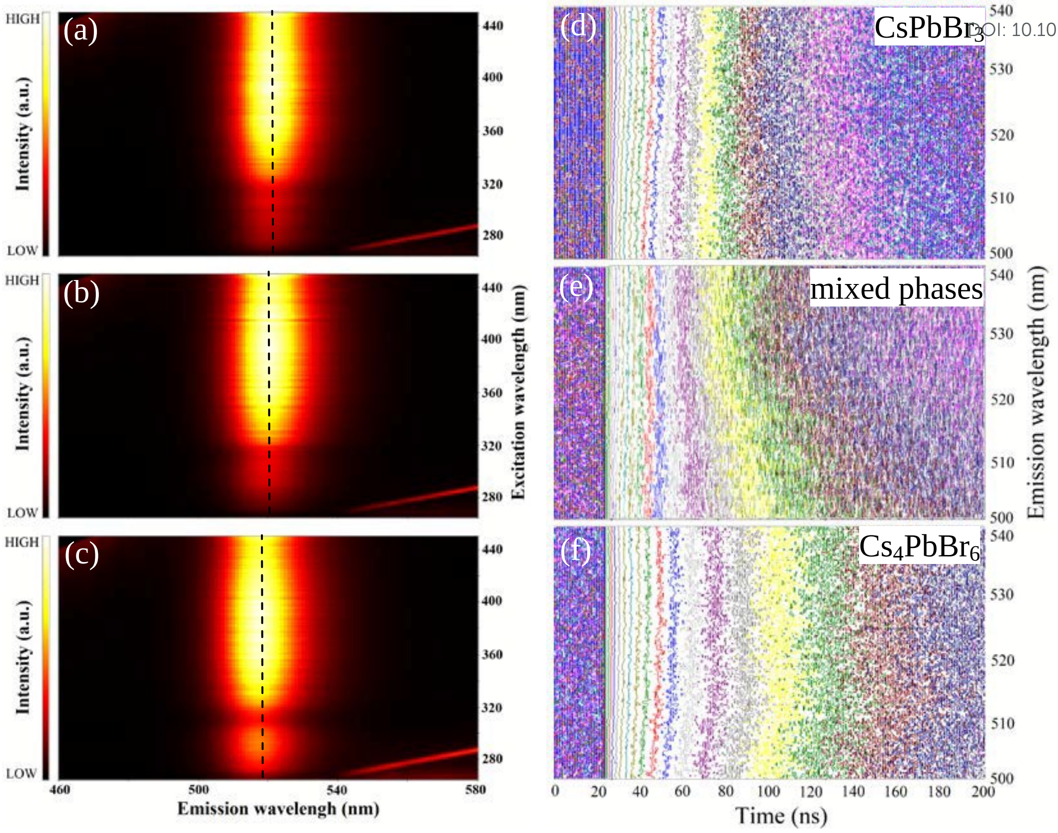

Figure 4. Two-dimensional excitation-emission mapping for the products prepared with (a) 0.2 mL OM & 0.1 mL OA (pure CsPbBr$_3$), (b) 1 mL OM & 0.5 mL OA (mixed phases), and (c) 2.5 mL OM & 1.25 mL OA (pure Cs$_4$PbBr$_6$) and (d-f) contour plots of time-resolved fluorescence data for the corresponding samples under the excitation of 375 nm picosecond laser.

Notably, PL of 0D perovskite-related Cs$_4$PbBr$_6$ is still a controversial theme. Though a large number of reports confirm PL of this kind of material, its origin opens to suspicion. Some researchers believed that PL was attributed to the presence of trace amount of highly fluorescent CsPbBr$_3$ NCs in the samples that cannot be detected by XRD measurements.[23,25] Meantime, a lot of investigations show that the band gap of Cs$_4$PbBr$_6$ is more than 3.8 eV due to the spatially isolated PbX$_6^{4-}$ octahedron in Cs$_4$PbBr$_6$ crystal, theoretically, no exciton emission in the visible range should be observed.[23] Herein, we further compare the optical performance of CsPbBr$_3$ and Cs$_4$PbBr$_6$ perovskite materials with the help of two-dimensional excitation-emission mapping as well as contour plots of PL decays. Evidently, both the CsPbBr$_3$ and Cs$_4$PbBr$_6$ products exhibit excitation independent emissions and phase conversion from CsPbBr$_3$ to Cs$_4$PbBr$_6$ results in the

View Article Online
DOI: 10.1039/C8DT00430G

blue shift of PL band (**Figure 4a-4c**), being consistent with the results shown in **Figure S2**. Time-resolved fluorescence was carried out to evaluate their fluorescent decay using time-correlated single-photon counting (TCSPC) methodology, as shown in **Figure 4d-4f**. Indeed, emission-wavelength-independent decays are detected for both $CsPbBr_3$ (**Figure 4d**) and Cs_4PbBr_6 (**Figure 4f**) samples and the former exhibit a shorter lifetime (~6 ns) than the latter (~13 ns); while for the mixed phases, emission-wavelength-sensitive decays are observed, and the average lifetime gradually decreases with increase of detecting luminescent wavelength from 500 nm to 540 nm, certainly evidencing the existence of two kind of fluorophors, i.e., their different emitting features of $CsPbBr_3$ and Cs_4PbBr_6.

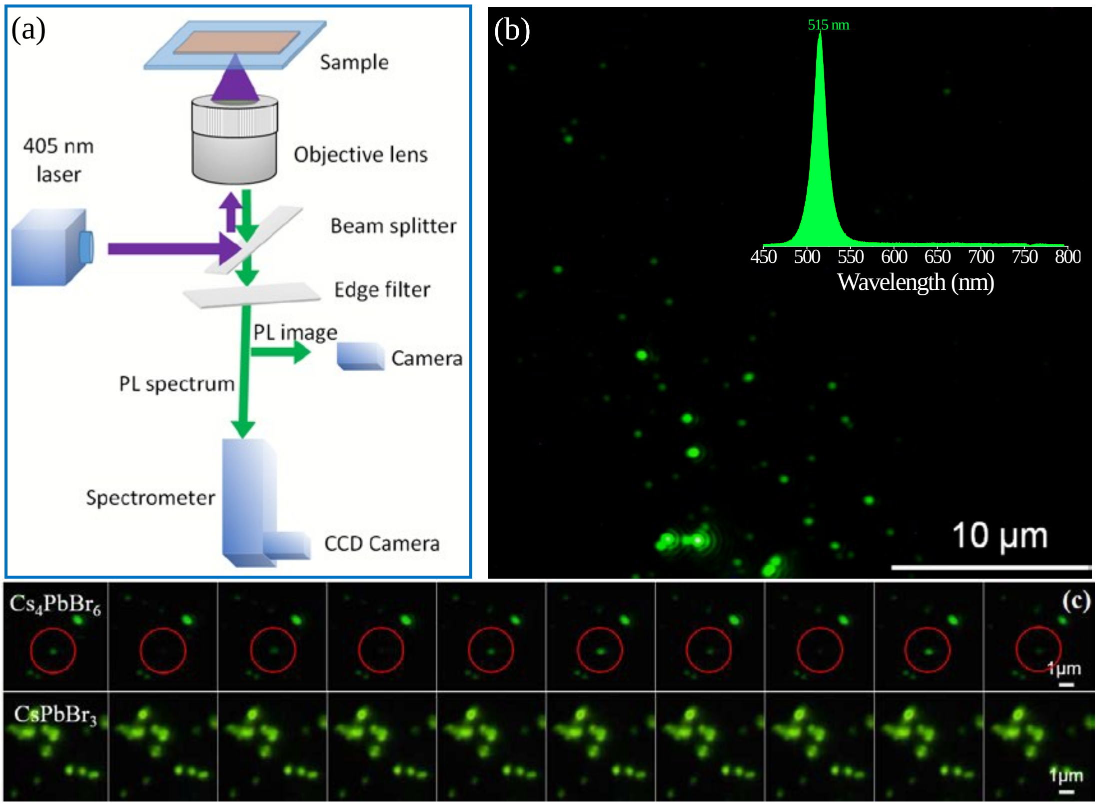

Figure 5. (a) Schematic illustration of the detection procedure to get emitting information of an individual particle achieve by a self-assembled instrument. (b) Fluorescence image of Cs_4PbBr_6 particles and the corresponding PL spectrum recorded on an individual particle. (c) Frequency flashing diagrams of Cs_4PbBr_6 particles and $CsPbBr_3$ ones over time (from left to right) with laser excitation wavelength of 405 nm; photo-blinking phenomenon for a typical Cs_4PbBr_4 particle is marked by red circles.

View Article Online
DOI: 10.1039/C8DT00430G

So far, optical measurements on the Cs_4PbBr_6 product were actually restricted in the ensemble system, which do not offer clear evidence of the identity of actual emitter. For the sake of resolving this issue, we focus on fluorescence imaging of Cs_4PbBr_6 at a single-particle level, as shown in the **Figure 5**. Using the single-molecule spectroscopy method, fluorescence from an individual molecule/particle can directly provide information beyond ensemble average, which has been applied to rationalize excited state migration processes in multichromophoric systems such as conjugated polymers, nanoparticles and aggregates.[41-43] Herein, PL measurements were conducted on a home-built Raman/PL system (**Figure 5a**), consisting of an inverted microscope (Ti eclipse, Nikon) and a Raman spectrometer (iHR320, Horiba) attached with an CCD detector (Syncerity, Horiba). A 405 nm laser was focused onto the sample using a 100×, 0.95 NA objective lens (Olympus) and then PL images were recorded by a visual camera. As evidenced in **Figure 5b**, each Cs_4PbBr_6 particle indeed shows a strong green emission and the obtained PL spectrum of an individual particle (inset of **Figure 5b**) exhibits a narrow emission band with peak wavelength located at 515 nm, being similar to the case of ensemble system. This result indicates that the luminescence is not significantly affected by the wide size distribution of Cs_4PbBr_6 particles. Similarly, intense green luminescence is also detectable from fluorescence image of $CsPbBr_3$ particle (**Figure S6**). It is worthy to mention that fluorescence intermittency can be easily observed for the present Cs_4PbBr_6 sample. Fluorescence intermittency has another name, blinking, describing as the stochastic switching of fluorescence intensity from an individual particle between extended periods of bright, intermediate stage and periods of dark under continuous laser excitation.[44-46] Frequency flashing diagrams of Cs_4PbBr_6 NCs and $CsPbBr_3$ ones over time are shown in **Figure 5c**. Obvious blinking can be observed for the Cs_4PbBr_6 particles while the

View Article Online
DOI: 10.1039/C8DT00430G

fluorescence intensity does not show significant changes for the $CsPbBr_3$ NCs with elongation of exposure time under the irradiation of 405 nm laser. The different photo-blinking behaviors for the prepared Cs_4PbBr_6 and $CsPbBr_3$ samples clearly confirm that the green emission of Cs_4PbBr_6 product is intrinsic and should not attribute to any impurity phase.

Not limited to the 3D structure perovskite $CsPbX_3$, 0D perovskite-related Cs_4PbX_6 can also tune over the visible spectral region by adjusting their composition (ratio of halide) in our investigation. Therefore, we have carried out a comparative study on these two types of perovskites. As we all know, 3D structure perovskite $CsPbX_3$ has been extensively investigated which crystallize in orthorhombic, tetragonal, and cubic polymorphs. Interestingly, we find that the present $CsPbX_3$ NCs mainly crystallize in the cubic phase (JPCDS No. 75-0412), only $CsPbBr_3$ exhibits monoclinic phase, which can be well distinguished by the split of diffraction peaks at 31^o and 48^o, as shown in **Figure 6a**. This phenomenon is in line with the recent results reported by Zeng and co-workers.[11] XRD patterns of all the Cs_4PbX_6 samples show a pure hexagonal phase (JPCDS No. 73-2478), and changing halogen composition in Cs_4PbX_6 will not modify the corresponding crystal structure (**Figure 6b**). Generally, the variation of composition is often accompanied by the change of lattice constant, which is reflected by the displacement of diffraction peaks in the XRD pattern. A partial magnification of XRD patterns of Cs_4PbX_6 is provided in **Figure 6c**. It can be clearly observed that the diffraction peaks gradually shift toward the low-angle direction with the change of halogen composition from Br/Cl to Br and finally to Br/I, verifying the successful substitution of Cl by Br and then by I in Cs_4PbX_6. We further investigated the optical properties of 3D structure perovskite $CsPbX_3$ and 0D perovskite-related Cs_4PbX_6. Similar to $CsPbX_3$, Cs_4PbX_6 can achieve multicolor luminescence by modulating

View Article Online
DOI: 10.1039/C8DT00430G

components of halogens. In the PL spectra of the $CsPbX_3$ products (**Figure 6d**), narrow emission bands, centered at 474 nm, 520 nm, 564 nm and 627 nm, with the corresponding halogen component ratios of Br:Cl=2:1, pure Br, Br:I=2:1, Br:I=1:2 respectively, are observed. In the same proportion of halogens, emission bands of Cs_4PbX_6, located at 468 nm, 515 nm, 574 nm, 633 nm, respectively, are detected (**Figure 6e**). The corresponding time-resolved fluorescence decay curves of $CsPbX_3$ and Cs_4PbX_6 with different halogen ratios are provided in **Figure 6f** and **6g**. As expected, the lifetime gradually increases with the substitution of Cl by Br and then I for both $CsPbX_3$ and Cs_4PbX_6 samples, and importantly, the lifetimes for Cs_4PbX_6 product are always longer than those of $CsPbX_3$ with the same halogen ratios (**Table S1**).

As previously reported by Q. A. Akkerman et. al.,[23] 0D peroskite-related Cs_4PbX_6, where the PbX_6^{4-} octahedrons are spatially separated, show large band gaps of 4.42, 4.00 and 3.44 eV for X=Cl, Br, I and cannot yield visible luminescence. However, the above-mentioned results certainly confirm that the observed multicolor emissions of Cs_4PbX_6 are indeed intrinsic. Herein, similar to the proposed mechanisms reported by M. De Bastiani and A. Samanta et. al.[17,24] we attributes the PL of Cs_4PbX_6 to charge carrier recombination from defect states to valence band, as schematically illustrated in **Figure 6h**. Such defect energy levels are believed to locate within the band gap and can capture electrons from conduction band, which are quite common for perovskite materials.[47,48] As perovskite semiconductors are ionic crystals and halogen ions are quite active, halogen-related defect states in Cs_4PbX_6 are proposed to act as the radiative recombination centers[17,24] in which excitons get trapped and then release to produce luminescence. With variation of halogen from Cl to Br and finally to I in Cs_4PbX_6, the changes in the positions of

View Article Online
DOI: 10.1039/C8DT00430G

valence/conduction bands will modify the energy gap between defect state and valence band, eventually leading to polychromatic emissions of Cs_4PbX_6.

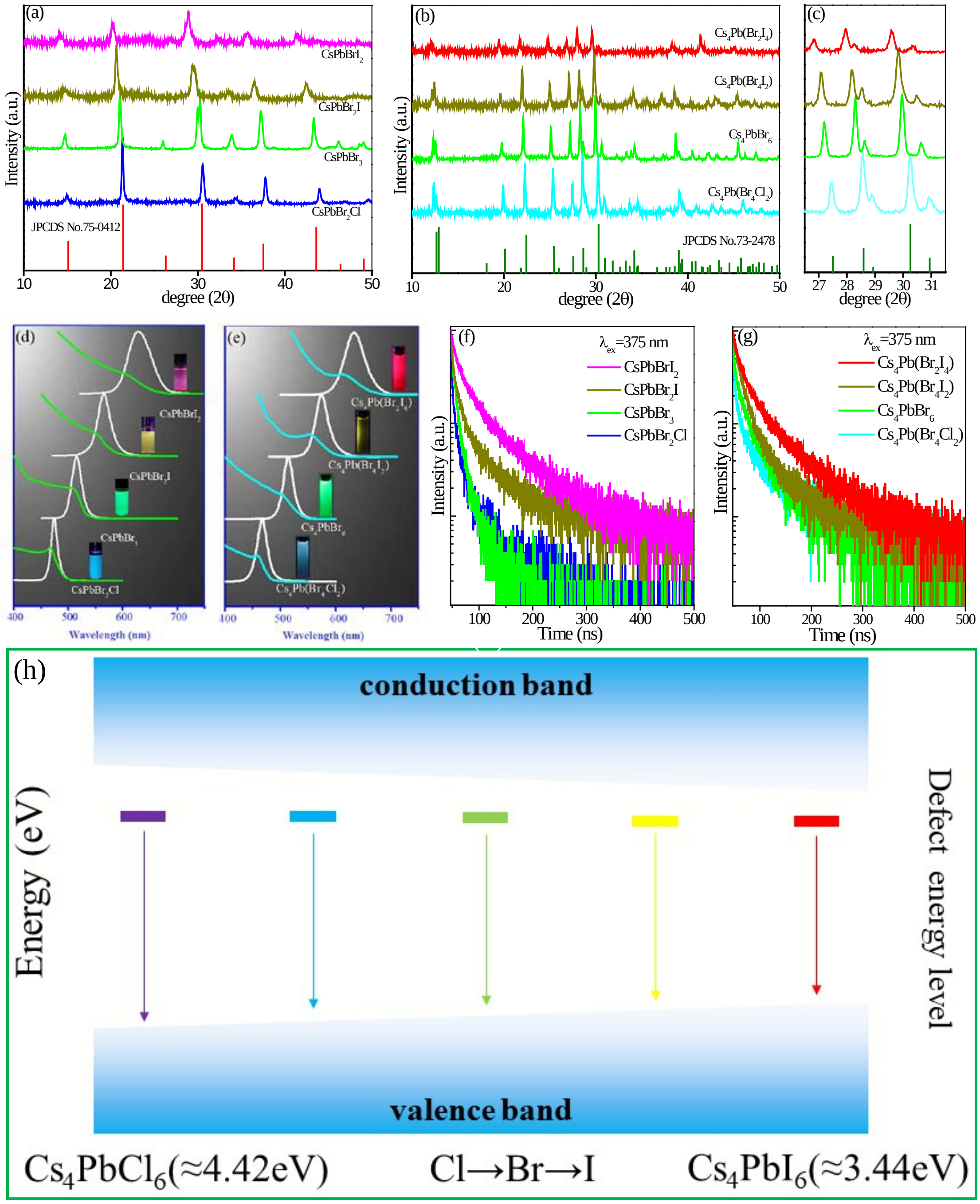

Figure 6. XRD patterns of (a) $CsPbX_3$ and (b) Cs_4PbX_6 (X=Cl/Br, Br, Br/I) samples. Bars represent standard diffraction data of cubic $CsPbBr_3$ (JPCDS No. 75-0412) and hexagonal Cs_4PbBr_6 (JPCDS No. 73-2478) crystals. (c) Enlarged XRD patterns for Cs_4PbX_6 (X=Cl/Br, Br, Br/I) products. The corresponding (d, e) absorption/PL spectra and (f, g) time-resolved fluorescence decay curves. Insets of (d, e) show the related luminescence photographs under the excitation of 365 nm UV lamp. (h) The possible mechanism for multi-color emissions of Cs_4PbX_6 samples, where halogen-related defect energy level is proposed to locate within band gap.

View Article Online
DOI: 10.1039/C8DT00430G

Conclusions

In summary, 3D perovskite $CsPbX_3$ and 0D perovskite-related Cs_4PbX_6 are successfully fabricated via a RT LASR strategy by simply transferring Cs^+, Pb^{2+}, and X^- precursors from a soluble good solvent to an insoluble bad one. Complete phase conversion from $CsPbX_3$ to Cs_4PbX_6 can be easily realized by modifying the content of surface ligands. PL, time-resolved fluorescence spectra and single-particle fluorescence images verify the intrinsic green luminescent nature of Cs_4PbBr_6. Importantly, multicolor luminescence is easily observed in the present Cs_4PbX_6 (X=Cl, Br, I) with the help of halogen substitution. We propose that the halogen-related defect states within band gap, acting as radiative recombination centers to capture excitons, should be responsible for the observed luminescence from Cs_4PbX_6. The present study, which provides a clear understanding of the structural and photophysical properties of the 0D perovskite-related Cs_4PbX_6 material, may be beneficial to promote their practical applications in the optoelectronic field.

Electronic Supporting Information

Table S1 and Figure S1-S6. Experimental details, the evaluated lifetimes, PLQYs, XRD patterns, temperature-dependent PL spectra, decay curves spectra, FTIR as well as PL image. This information is available free of charge via the Internet at http://pubs.acs.org/.

Author Information

Corresponding author

*E-Mail: dqchen@hdu.edu.cn (D. Q. Chen)

View Article Online
DOI: 10.1039/C8DT00430G

Acknowledgements

This research was supported by Zhejiang Provincial Natural Science Foundation of China (LR15E020001), National Natural Science Foundation of China (51572065), and 151 Talent's Projects in the Second Level of Zhejiang Province.

Notes

The authors declare no competing financial interest.

References

(1) H. Cho, S.-H. Jeong, M. H. Park, Y.-H. Kim, C. Wolf, C.-L. Lee, J. H. Heo, A. Sadhanala, N. Myoung, S. Yoo, S. H. Im, R. H. Friend, T. W. Lee, *Science*, 2015, **350**, 1222-1225.

(2) P. Ramasamy, D. H. Lim, B. Kim, S. H. Lee, M. S. Leeb, J. S. Lee, *Chem. Commun.*, 2016, **52**, 2067-2070.

(3) Z. K. Tan, R. S. Moghaddam, M. L. Lai, P. Docampo, R. Higler, F. Deschler, M. Price, A. Sadhanala, L. M. Pazos, D. Credgington, F. Hanusch, T. Bein, H. J. Snaith, R. H. Friend, *Science*, 2015, **350**, 1222-1225.

(4) J. H. Li, L. M. Xu, T. Wang, J. Z. Song, J. W. Chen, J. Xue, Y. H. Dong, B. Cai, Q. S. Shan, B. N. Han, H. B. Zeng, *Adv. Mater.*, 2016, **29**, 1603885.

(5) A. Swarnkar, A. R. Marshall, E. M. Sanehira, B. D. Chernomordik, D. T. Moore, J. A. Christians, T. Chakrabarti, J. M. Luther, *Science*, 2016, **354**, 92-95.

(6) A. Kojima, K. Teshima, Y. Shirai, T. Miyasaka, *J. Am. Chem. Soc.*, 2009, **131**, 6050-6051.

(7) J. H. Noh, S. H. Im, J. H. Heo, T. N. Mandal, S. I. Seok, *Nano Lett.*, 2013, **13**, 1764-1769.

(8) J. H. Heo, S. H. Im, J. H. Noh, T. N. Mandal, C.-S. Lim, J. A. Chang, Y. H. Lee, H. J. Kim, A. Sarkar, M. K. Nazeeruddin, M. Grätzel, S. Seok, *Nat. Photonics*, 2013, **7**, 486-491.

(9) Y. Wang, X. M. Li, X. Zhao, L. Xiao, H. B. Zeng, H. D. Sun, *Nano Lett.*, 2016, **16**, 448-453.

(10) L. Protesescu, S. Yakunin, M. I. Bodnarchuk, F. Krieg, R. Caputo, C. H. Hendon, R. X. Yang, A. Walsh, M. V. Kovalenko, *Nano Lett.*, 2015, **15**, 3692-3696.

(11) X. M. Li, Y. Wu, S. L. Zhang, B. Cai, Y. Gu, J. Z. Song, H. B. Zeng, *Adv. Funct. Mater.*, 2016, 26, 2435-2445.

(12) F. Zhang, H. B. Zhong, C. Chen, X. M. Wu, X. G. Hu, H. L. Huang, J. B. Han, B. S. Zou, Y. P. Dong, *ACS Nano*, 2015, **9**, 4533-4542.

(13) C. Sun, Y. Zhang, C. Ruan, C. Y. Yin, X. Y. Wang, Y. D. Wang, W. W. Yu, *Adv. Mater.*, 2016, **28**, 10088-10094.

(14) A. F. Wang, X. X. Yan, M. Zhang, S. B. Sun, M. Yang, W. Shen, X. Q. Pan, P. Wang, Z. T. Deng, *Chem. Mater.*, 2016, **28**, 8132-8140.

(15) K. P. Marshall, M. Walker, R. I. Walton, R. A. Hatton, *Nat. Energy*, 2016, **1**, 16178.

(16) D. Q. Chen, Z. Y. Wan, X. Chen, Y. J. Yuan, J. S. Zhong, *J. Mater. Chem. C.*, 2016, **4**, 10646-10653.

(17) S. Seth, A. Samanta, *J. Phys. Chem. Lett.*, 2017, **8**, 4461-4467.

View Article Online
DOI: 10.1039/C8DT00430G

(18) B. Saparov, D. B. Mitzi, *Chem. Rev.*, 2016, **116**, 4558-4596.

(19) S. B. Sun, D. Yuan, Y. Xu, A. F. Wang, Z. T. Deng, *ACS Nano*, 2016, **10**, 3648-3657.

(20) X. L. Zhang, B. Xu, J. B. Zhang, Y. Gao, Y. J. Zheng, K. Wang, X. W. Sun, *Adv. Funct. Mater.*, 2016, **26**, 4595-4600.

(21) X. S. Tang, Z. P. Hu, W. Yuan, W. Hu, H. B. Shao, D. Han, J. F. Zheng, J. Hao, Z. G. Zang, J. Du, Y. X. Leng, L. Fang, M. Zhou, X. Tang, *Adv. Opt. Mater.*, 2017, **5**, 1600788.

(22) M. C. Weidman, M. Seitz, S. D. Stranks, W. A. Tisdale, *ACS Nano*, 2016, **10**, 7830-7839.

(23) Q. A. Akkerman, S. Park, E. Radicchi, F. Nunzi, E. Mosconi, F. D. Angelis, R. Brescia, P. Rastogi, M. Prato, L. Manna, *Nano Lett.*, 2017, **17**, 1924-1930.

(24) M. D. Bastiani, I. Dursun, Y. Zhang, B. A. Alshankiti, X. Miao, J. Yin, E. Yengel, E. Alarousu, B. Turedi, J. M. Almutlaq, M. I. Saidaminov, S. Mitra, I. Gereige, A. AlSaggaf, Y. Zhu, Y. Han, I. S. Roqan, J. Bredas, O. F. Mohammed, O. M. Bakr, *Chem. Mater.*, 2017, **29**, 7108-7113.

(25) M. I. Saidaminov, J. Almutlaq, S. Sarmah, I. Dursun, A. A. Zhumekenov, R. Begum, J. Pan, N. Cho, O. F. Mohammed, O. M. Bakr, *ACS Energy Lett.*, 2016, **1**, 840-845.

(26) Y. Zhang, M. I. Saidaminov, I. Dursun, H. Yang, B. Murali, E. Alarousu, E. Yengel, B. A. Alshankiti, O. M. Bakr, O. F. Mohammed, *J. Phys. Chem. Lett.*, 2017, **8**, 961-965.

(27) Y. Wang, D. J. Yu, Z. Wang, X. M. Li, X. X. Chen, V. Nalla, H. B. Zeng, H. D. Sun, *small*, 2017, **13**, 1701587.

(28) C. Weerd, J. Lin, L. Gomez, Y. Fujiwara, K. Suenaga, T. Gregorkiewicz, *J. Phys. Chem. C.*, 2017, **121**, 19490-19496.

(29) K. X. Huang, D. M. Li, L. Yang, S. Liu, F. Yang, *J. Alloys Compd.*, 2017, **5**, 244-252.

(30) Q. A. Akkerman, V. D'Innocenzo, S. Accornero, A. Scarpellini, A. Petrozza, M. Prato, L. Manna, *J. Am. Chem. Soc.*, 2015, **137**, 10276-10281.

(31) Y. Tong, E. Bladt, M. F. Aygler, A. Manzi, K. Z. Milowska, V. A. Hintermayr, P. Docampo, S. Bals, A. S. Urban, L. Polavarapu, J. Feldmann, *Angew. Chem. Int. Ed.*, 2016, **55**, 1-7.

(32) M. Chen, Y. Zou, L. Wu, Q. Pan, D. Yang, H. Hu, Y. Tan, Q. Zhong, Y. Xu, H. Liu, B. Sun, Q. Zhang, *Adv. Funct. Mater.*, 2017, **23**, 1701121.

(33) D. Q. Chen, X. Chen, Z. Y. Wan, G. L. Fang, *ACS Appl. Mater. Interfaces*, 2017, **9**, 20671-20678.

(34) A. G. Dong, X. C. Ye, J. Chen, Y. J. Kang, T. Gordon, J. M. Kikkawa, C. B. Murray, *J. Am. Chem. Soc.* 2011, **133**, 998-1006.

(35) J. Cho, H. Jin, D. G. Sellers, D. F. Watson, D. H. Son, S. Banerjeea, *J. Mater. Chem. C.*, 2017, **34**, 1-10.

(36) I. Moreels, Y. Justo, B. D. Geyter, K. Haustraete, J. C. Martins, Z. Hens, *ACS Nano*, 2011, **5**, 2004-2012.

(37) C. R. Bealing, W. J. Baumgardner, J. J. Choi, T. Hanrath, R. G. Hennig, *ACS Nano*, 2012, **6**, 2118-2127.

(38) U. Thumu, L. Houben, H. Cohen, M. Menahem, I. Pinkas, L. Avram, T. Wolf, A. Teitelboim, M. Leskes, O. Yaffe, D. Oron, M. Kazes, *Chem. Mater.*, 2018, **30**, 84-93.

(39) L. Yang, D. M. Li, C. Wang, W. Yao, H. Wang, K. X. Huang, *J. Nanopart. Res.* **2017**, 19, 258.

(40) P. Politzer, J. S. Murraya, T. Clark, *Phys. Chem. Chem. Phys.*, 2010, **12**, 7748-7757.

(41) H. Lin, R. Camacho, Y. Tian, T. E. Kaiser, F. Wùrthner, I. G. Scheblykin, *Nano Lett.*, 2010,

View Article Online
DOI: 10.1039/C8DT00430G

10, 620-626.

(42) H. Lin, S. R. Tabae, D. Thomsson, O. Mirzov, P. O. Larsson, I. G. Scheblykin, *J. Am. Chem. Soc.*, 2008, **130**, 7042-7051.

(43) X. Zhou, N. M. Andoy, G. Liu, E. Choudhary, K. S. Han, H. Shen, P. Chen, *Nat. Nanotechnology*, 2012, **7**, 237-241.

(44) M. Nakamura, S. Ozaki, M. Abe, T. Matsumotob, K. Ishimuraa, *J. Mater. Chem.*, 2011, **21**, 4689-4695.

(45) T. D. Krauss, J. J. Peterson, *J. Phys. Chem. Lett.*, 2010, **1**, 1377-1382.

(46) Y. Tian, A. Merdasa, M. Peter, M. Abdellah, K. Zheng, C. S. Ponseca, T. Pullerits, A. Yartsev, V. Sundstrom, I. G. Scheblykin, *Nano Lett.*, 2015, **15**, 1603-1608.

(47) J. M. Ball, A. Petrozza, *Nat. Energy*, 2016, 16149.

(48) J. Kang, L. W. Wang, *J. Phys. Chem. Lett.*, 2017, **8**, 489-493.

View Article Online
DOI: 10.1039/C8DT00430G

TOC